Engineering Failure Analysis 68 (2016) 122–131

Contents lists available at ScienceDirect

Engineering Failure Analysis

journal homepage: www.elsevier.com/locate/engfailanal

Cracking mechanisms in large size ingots of high nickel content low alloyed steel

Matthieu Bitterlin [a,*], Abdelhalim Loucif [a], Nicolas Charbonnier [a], Mohammad Jahazi [a], Louis-Philippe Lapierre-Boire [b], Jean-Benoît Morin [b]

[a] École de technologie supérieure, Département de Génie Mécanique, 1100, rue Notre-Dame Ouest, Montréal, QC H3C 1K3, Canada
[b] Sorel Forge Inc., 100 McCarthy, Saint-Joseph-de-Sorel, QC, J3R 3M8, Canada

Authors' accepted manuscript
Article published in *Engineering Failure Analysis* vol. 68 (2016)
https://doi.org/10.1016/j.engfailanal.2016.05.027

Cracking mechanisms in large size ingots of high nickel content low alloyed steels

Matthieu Bitterlin [a*] (matthieubitterlin@gmail.com), Abdelhalim Loucif [a], Nicolas Charbonnier [a], Mohammad Jahazi [a], Louis-Philippe Lapierre-Boire [b], Jean-Benoît Morin [b]

[a] École de technologie supérieure, Département de Génie Mécanique, 1100, rue Notre-Dame Ouest Montréal, QC, H3C 1K3, Canada

[b] Sorel Forge Inc., 100 McCarthy, Saint-Joseph-de-Sorel, QC, J3R 3M8, Canada

Authors' accepted manuscript
Article published in *Engineering Failure Analysis* vol. 68 (2016)
https://doi.org/10.1016/j.engfailanal.2016.05.027

Abstract

This study is focused on determining the possible root causes for cracking after open die forging of large size ingots made of high nickel medium carbon low alloy steels. Optical and scanning electron microscopies as well as Energy Dispersion Spectroscopy (EDS) were used to examine the microstructure of the samples taken out of a cracked forged ingot. The large size of the samples permitted to investigate microstructure at different locations at the surface and in depth. Chemical analysis revealed chromium and oxygen enrichment at the grain boundaries. Grain size measurement indicated clear differences between “clean” surface zones and cracked ones, and between surface and in depth regions. The analyses indicated that fracture phenomena may be due to abnormal grain size which promotes oxide penetration into grain boundaries, resulting in their embrittlement and cracking upon cooling.

Keywords: cracks, intergranular oxidation, microalloyed steel, abnormal grain growth.

1. Introduction

High-strength low alloy (HSLA) microalloyed steels are used in petrochemical industry, principally as pipes and equipment needed to dig cores in the ground to extract bituminous soil [1, 2]. Conditions of extraction require high mechanical properties such as hardness, toughness, and good wear resistance that can be obtained by using medium carbon low alloyed steels which, in addition to elements under 0.1 wt.% such as vanadium, niobium or titanium, contain nickel and chromium amounts of about 2 wt.% [3]. These steels are formed by ingot casting followed by multiple open-die forging passes at temperatures above 1000°C. Such steels have good hardenability, air cooling after forging and tempering produces a bainitic microstructure through the thickness of the forged ingot. Following the forging process, normalizing, quenching and tempering

operations produce a complex microstructure composed of tempered martensite and bainite as well as various types of carbides [3].

In recent years, industrial demands for large size ingots have increased continuously. One of the challenges in forging of large size ingots is the occurrence of cracking phenomena which have been observed during the forging process or during the post forge heat treatment operations [4]. Such failures can be the result of different mechanisms, such as segregation, precipitates and/or abnormal large grain size.

Segregation can lead to some discontinuities of properties in the microstructure and therefore of forgeability, due to local compositional changes [5, 6]. Barrela et al. [7] reported that in NiCrMoV steel segregated and banded microstructures modify the austenite grain size, resulting in increased sensitivity to brittleness of the alloy. The extent of the segregation phenomena increases in large steels ingots of highly alloyed steels and is not eliminated during reheating and/or forging operations [8-10].

Many cases of failure and debits in mechanical properties are the result of the formation of secondary phases, such as sulfides at grain boundaries [4, 11-13. For instance, it is well known that MnS particles are a main source of cracking in steels, since they are formed at grain boundaries and can impact both transverse and longitudinal toughness of steels [4]. Thus, controlling the formation and shape of sulfides is important in order to minimize their influence on mechanical properties. This is generally achieved by adding silicon or calcium during casting [4, 14].

Likewise, grain size has a direct impact on toughness. Abnormal large grains have smaller grain boundary length and fewer triple points when compared to small grain microstructures. This implies high ductility of the alloy but diminishes the resistance of the steel to impact or stress and can be source of cracking, whether during forging heat treatment processes [4, 14]. On the other hand, it has been reported that during hot compression of NiCrMoV medium carbon steels dynamic recrystallization may takes place which brings grain refinement to the structure [15-17]. It has been also reported that dynamic precipitation, notably of carbonitrides may also occur, hindering the

occurrence of abnormal grain growth [17]. Therefore the presence of abnormal large grain size in such steels is not generally expected during the forging process.

However, recent studies report failures in medium carbon microalloyed steels containing chromium and nickel in proportions up to 2 wt.%. Specifically, Barsom [18] reported cracking in forged AISI 4340 steel and associated it to overheating and incipient melting at grain boundaries. He et al. [19] reported a similar finding in NiCrMoV steel, but concluded that cracking was caused by heavy deformation ratio and high strain rates employed during the forging process. The formation of silicon and iron oxides at the interface of the oxide layer and the steel (fayalite) has been also associated with intergranular corrosion inducing cracking during forging in nickel-added steels [20]. A cohesive picture cannot therefore be drawn from the above mentioned studies on the root causes for the observed cracking. This could mainly be due to the lack of a comprehensive study addressing the different sources of cracking in a single alloy.

The main objective of the present study is to investigate the different mechanisms at the origin of crack formation during forging of large size ingots made of Ni rich medium carbon low alloy steels. For this purpose, a wide range of characterization techniques were used to reveal grain size, chemical composition, phase identification, phase distribution, etc. at the base of the cracks and deep in the material. Thermodynamic analysis was used to determine formation of phases in the steel and correlate it with experimental findings. Finally, the forging process was also analysed to understand its impact on microstructure evolution and proportions of phases.

2. Experimental procedure

Samples were collected and provided by Sorel Forge Inc., Quebec, Canada. The nominal composition of the cracked steel investigated in this study is given in Table 1. The manufacturing process consisted of 56 inches of diameter (142cm) and 20 tons ingot

casting, 7 passes open die forging and heat treatment operations consisting of normalization, quenching and tempering. The forged component showed cracks at the end of the normalizing heat treatment process carried out at 900°C. The process had followed standard forging practices in place for similar components and no case of overheating or abnormal deformation conditions was reported.

The surface of the component was machined in order to remove surface oxides and proceed to ultrasonic and dye penetrant non-destructive analyses. Fig. 1a shows the component after dye penetrant testing where a large number of cracks can be observed (in red). Also specified in Fig. 1a, is the location on the forged ingot where a large block was machined out. Fig. 1b presents the collected block and its dimensions. Four smaller specimens, S1 to S4, were cut from different locations of the block as indicated in Fig. 1c. The specimens were selected from regions within the cracked zone, in its vicinity, very far from it in the non-affected zone, and near the surface but far from the crack. The specimens were individually mounted and polished from the 200 to 1200 grade SiC paper, then finished with 1µm diamond grain paste. Clear revealing of the prior austenite grain boundaries is an experimental challenge in these heavily forged steels. A large number of solutions recommended in the literature [21] were used without success. A methodology using a modified solution containing Picral was developed in the present investigation: an aqueous solution of 10g of picric acid, with few drops of Zephiran chloride used as wetting agent was heated to 83°C (181°F). Samples were immersed for about 1 minute and 45 seconds, cleaned with water then methanol in order to remove picric residues. After drying, surface passivation of specimens was gently removed applying cotton under water. Crack base was revealed using Beaujard reagent for about 4 minutes at room temperature. The reagent is constituted of a saturated aqueous picric acid solution with few drops of sodium alkyl sulfonate used as wetting agent. Literature highlights that Beaujard's reagent revealing austenite grains boundaries in metastable microstructures [22]. Microstructural observations were carried out on confocal microscope Olympus LEXT 4100. Grain size determination was made according to ASTM E12-112 standard and the size distribution was obtained using

image analyzer software MIP 4.2. Investigations were done on SEM Hitachi TM3030 at 15kV equipped with EDS capability for detailed microstructure and chemical analysis of cracks, oxide layers and inclusions. X-ray diffraction experiments were conducted on X'Pert³ MRD PANalytical using Cu Kα radiation with a step size (2-theta) of 0,0330. Thermo-Calc thermodynamic software was used to predict the presence of phases between 500°C and 1600°C of the investigated steel, and correlate it with experimental findings.

3. Results

Optical microscopy observations, Fig. 2a, revealed the presence of a large number of secondary cracks bifurcated from the large size cracks. Most of the latter follow grain boundaries while secondary cracks were both inter or transgranular. Fig. 2a shows a macrograph of the S4 specimen where large size cracks are visible. As it can be seen all appear initiated from the surface and developed along the grain boundaries. The main fracture visible in Fig. 1b, can also be seen at the extreme left of the specimen. Microscopic examination of near surface region of a large number of samples revealed clear differences in the orientations of bainite laths and severe contrast changes from one region to another, which are characteristic of large prior austenite grain sizes. Fig. 2b is a high magnification micrograph of the surface of the S4 specimen. It can be seen that oxides penetration has occurred within the grain boundaries resulting in the formation of voids and grain separation in some locations.

A mean grain size of about 500µm was calculated in the surface zone adjacent to a main crack. Results of grain size measurements for S1 to S4 specimens are reported in Table 2. Examination of the data indicates that very large grains are present at the surface of the sample. Microscopic observations, Fig. 3, revealed bainitic microstructure, recognizable by plates and laths. Intergranular cracks on large grain zones are also visible in Fig. 3. It is also important to note that the average grain size is significantly

larger near the main crack than in a non-cracked surface zone, indicating that a grain growth process has taken place in the vicinity of cracked zones. Furthermore, Table 2 and Fig. 3 show that in the sample far from the surface (S2 specimen, 8cm deep), grains are smaller by a factor of more than 10 compared to the surface ones.

Simulations of phases formed in the current steel between 500°C and 1600°C were carried out using Thermo-Calc, and the results are presented in Fig. 4a and Fig. 4b. From these figures, A3 and liquidus equilibrium transformation lines were determined. The thermodynamic analysis reveals little proportions of second phases in this steel. Detailed examination of these precipitates, shown in Fig. 4b, reveals preferential presence of M_xC_y carbides, including carbide-forming elements such as chromium and vanadium, and little proportion of other carbides. Much lower fractions of MnS and AlN, the latter only reaching 0,029%, are also revealed by the Thermo-Calc analysis. X-ray diffraction of the first oxide layer is presented in Fig. 5. It reveals the presence of both magnetite and nickel-iron spinel in the first oxide layer. Micrograph observations coupled with EDS elemental analysis on second phases of the oxide layer revealed a network of high nickel and iron oxide.

SEM photograph of the base of an open crack is reported in Fig. 6a. The Beaujard's reagent reacts with oxide scale and depleted carbon zones and results in white etching for the grain boundaries around the base of the crack. In Fig. 6, the boundaries of the grains are also highlighted. The average size of these grains is very close to the one found for the S2 specimen (see Table 2). Also in Fig. 6, certain boundary precipitates are visible around the crack. EDS elemental analysis of these precipitates (Fig. 6b, c, d and e) revealed the presence of a mixture of chromium and manganese oxide in the composition of the precipitates. Line scan EDS analysis of an oxidized crack is shown in Fig. 7. It reveals a high-chromium content in the oxide layer on both sides of the crack. Similar observations were made on other cracks, confirming that chromium enrichment is present in the oxide layers at the vicinity of the cracked regions.

4. Discussion

The large grain size at the surface, and near the main crack as shown in Figs. 2a, 2b and 3a are probably related to the seven passes of forging. It is well known that precipitates like carbides and nitrides can reduce the grain growth and the size of recrystallized grains during deformation or reheating [23-25]. Chromium and molybdene carbides are the most likely precipitates to be produced in the investigated steel, since they have low enthalpy of nucleation and growth [3, 26]. However despite Thermo-Calc simulation (Fig. 4b) showing the presence of nearly 4% M_7C_3 composed mostly of chromium; microscopic observations did not show carbides at the grain boundaries and/or inside grains; however, it is possible that due to their small sizes the carbides have been washed out during the hot picric acid etching process (Fig. 3b). It is worth mentioning that, Thermo-Calc Simulation results (Fig. 4b) are in agreement with previous studies on carbides formation in low alloyed microalloyed steels [27].

Apart from carbides, Thermo-Calc analysis indicated also that very low proportions of manganese sulfides (0,017%) or AlN (0,029%) may be formed under the consideered conditions. The investigated steel has been treated with calcium before casting, to control the shape and reduce the size of MnS and AlN precipitates in the microstructure [14]. During metallographic and multi-element chemical analysis, occasional presence of spheroïdal MnS was detected near the cracks, confirming the prediction of Thermo-Calc simulation shown in Fig. 4b as well as successful calcium treatment process. The above finding are in contrast to some reported results [4, 12, 28] which associated failures to sulfides inclusions. Furthermore, the presence of AlN was not detected during analyses. This is in agreement with the findings of Connolly *et al.* [5] on ductility drop during casting of P20 steel and 3.5Ni steel.

A network of high nickel content oxides was observed in the oxide layer (Fig. 5). Song *et al*. [20] suggested that zones close to the surface of a high Si containing steel might have a lower nickel content than the base steel composition but did not report the formation of a network. However, in the present work, EDS analyses didn’t reveal any nickel

depletion in the surface zone. Further analyses should be then undertaken to understand the formation of such network of oxides in the surface region of high nickel medium carbon low alloy steels. The presence of chromium and manganese oxides very close to the edges of the cracks (Fig. 6b, c, d and e) suggests that there is no barrier stopping or delaying grain growth during reheating. The formation of these oxides is probably the result of multiple reheating and cooling cycles during the forging process.

The high temperatures of forging and reheating stages govern the diffusion of many elements, including manganese and chromium. The latter has a diffusion coefficient hundred times higher than iron at high temperatures [29]. The same situation holds for manganese whose diffusion in oxides is much faster than chromium or iron [30]. Such high diffusion rates could explain the formation of multi-element oxides at the base of the cracks (Fig. 6 b, c, d and e) despite their high enthalphy of formation [31-33]. These oxides appear at the grain boundaries near the base of the cracks. Etching of the cracked area with Beaujard's reagent [22] revealed the presence of a 10µm oxide layer and a zone of about 1µm wide depleted grains boundaries near the crack (Fig. 6a). However, the grain size at the base of the crack is very small and is in the range of 15-20µm. Therefore, oxide penetration in the material is probably the main source for crack growth in the regions far from the surface. This finding is in contrast with the origin of near surface cracks which appears to be related to the abnormal grain size in these regions (Fig. 2b and Fig. 3a). Metallographic observations of etched specimens (Fig. 6a) confirm that oxides are formed and grow through grain boundaries, with different intensities, depending on the crack size and the distance from the surface. The obtained results are in agreement with those reported by other authors [34, 35]. The fragilization brought to the material by the formation of these oxides is probably one of the root causes for crack growth in the investigated steel. It is generally considered that the region close to the surface of the slab is characterized by a decarburized zone as well as depletion from some alloying elements [36]. However, in contrast to the intergranular corrosion phenomenon observed in stainless steels [12], no indication of depletion of chromium near cracks or next to the chromium oxide in the vicinity of

cracks was observed in the present work. This probably indicates that chromium oxide growth rate is higher than it's diffusion rates under the investigated processing conditions. Fig. 7 shows the EDS cross line scan analysis of a crack containing significantly high amounts of chromium oxide while no change is observed in the vicinity of the crack.

During the cogging process, the material is deformed at high temperatures. Upon the application of a critical strain, dynamic recrystallization may take place [24, 25]. If this condition is not respected, rapid grain growth may result. The presence of large grains impact negatively the toughness and the ductility of the steel. Similarly, multiple reheating operations after deformation can induce grain growth near the surface of the forged ingot thereby increasing the propensity of the material for cracking. Also insufficient deformation, e.g. during cogging steps, may not provide enough deformation energy to the material to recrystallize. The recrystallization could be dynamic, i.e. during the application of deformation or static, i.e. during the interpass time between each blow or reheating stages.

It is well known that strain rate and temperature are the main parameters that control grain growth during static and dynamic recrystallization [7-9, 37]. The cogging steps are characterized by fast but small deformations, which therefore mainly affect the region close to the surface of the material. Also, the ingot surface, particularly in the case of large size ingots, is the zone that will be much affected during the reheating process. Thus ingot surface will be the most favourable zone where and static recrystallization (assuming that the critical strain for recrystallization has been attained) or grain growth could take place [24, 25]. Several authors [24, 25] have highlighted the sensitivity to grain growth under insufficient deformation and/or high temperature processing as in the absence of critical conditions for recrystallization, temperature and holding time are the main parameters governing grain growth. The axial shape of grains in Fig. 2a, 2b and Fig. 3 suggested recrystallization occurred during the forging process, and then surface grains grow during normalizing heat treatment. The obtained results are in agreement

with those reported on 26NiCrMoV11.5 High Strength Steel by Barella et al. [7] who observed that even few hours added to the common practiced holding time can have significant influence on grain size and the morphology of the grain boundaries, especially at high temperatures.

Based on the above observations and analysis of the results, it can be said that holding time either during the normalizing heat treatment or the intermediate reheating stages between forging passes, must be controlled in order to minimize grain growth in the surface zone of the forged component and minimize the cracking susceptibility of the investigated alloy.

5. Conclusions

The cracking phenomena observed in medium carbon high nickel content low alloy steel has been investigated with micrograph observations and elemental analysis, completed with simulation in this work, and several important points are noted:

1) The abnormal grain size measured at the surface of the investigated steel is probably the result of two phenomena :
    a. Long holding time during the normalizing heat treatment process leading to abnormal grain growth in the surface zone of the forged component.
    b. Insufficient deformation conditions during cogging steps of open-die forging process to induce recrystallization in these zones resulting in substantial grain growth during subsequent reheating stages.
2) The presence of high content chromium oxides at the grain boundaries in the vicinity of the base of cracks was demonstrated in the present investigation.
3) Two possible and concomitant mechanisms of cracking are possible in the investigated steel :

a. Abnormal grain size is at the origin of cracking at and near the surface regions;
b. The presence of grain boundary high chromium content oxides at the base of the cracks far from the surface despite the small grain size in these regions.

4) The root cause of cracking was identified as being the overdue furnace holding time during the normalizing process. A more stringent control over the normalizing heat treatment time is therefore required to avoid cracking in these large size components made of high Ni content medium Carbon low alloy steels.

References

[1] N. Narimani, B. Zarei, H. Pouraliakbar, G. Khalaj. Predictions of corrosion current density and potential by using chemical composition and corrosion cell characteristics in microalloyed pipeline steels. Measurement. 62 (2015) 97-107.

[2] W. B. Lee, S. G. Hong, C. G.Park, K. H. Kim, S. H. Park, Carbide precipitation and high temperature strength of hot rolled containing Cr and Mo fire resistant steels J. Korean Inst. Metal & Mater. 38(3) (2000) 420-426.

[3] H. Bhadeshia, R. Honeycombe, Steels - Microstructure and Properties (3rd Edition), Elsevier, 2006.

[4] W.T. Becker, R.J. Shipley, Manufacturing Aspects of Failure and Prevention, ASM Handbook, Volume 11 - Failure Analysis and Prevention, ASM International, 1985, 2002, pp. 81-102.

[5] B.M. Connolly, J. Paules, A. DeArdo. The effects of composition and thermal path on hot ductility of forging steels. Metall Ital. (2015) 3-9.

[6] R.N. Penha, J. Vatavuk, A.A. Couto, S.A.D. Pereira, S.A. de Sousa, L.D. Canale. Effect of chemical banding on the local hardenability in AISI 4340 steel bar. Engineering Failure Analysis. 53 (2015) 59-68.

[7] S. Barella, A. Gruttadauria, C. Mapelli, D. Mombelli, C.L. Fanezi, F. Fioletti, et al. Effect of Heat Treatment and of Primary Austenite Grain Size on the Minimum Size of Detectable Defect on 26NiCrMoV11.5 High Strength Steel. Advanced Engineering Materials. 16 (2014) 103-111.

[8] M. Wu, J. Li, A. Kharicha, A. Ludwig, Using a Three-Phase Mixed Columnar-Equiaxed Solidification Model to Study Macrosegregation in Ingot Castings: Perspectives and Limitations, Proceedings of the 2013 International Symposium on Liquid Metal Processing and Casting (LMPC), John Wiley & Sons, 2013, pp. 171-180.

[9] R. Nadella, D. Eskin, Q. Du, L. Katgerman. Macrosegregation in direct-chill casting of aluminium alloys. Progress in Materials Science. 53 (2008) 421-480.

[10] E.J. Pickering, Macrosegregation in Steel Ingots: The Applicability of Modelling and Characterisation Techniques, Isij International, 2013, pp. 935-949.

[11] J. R. Shant, B. K. Pandey, R. K. Goyal, T. S. Kathayat, Failure Analysis of Cracks Formed at Extrados of Bend Pipe of API 5L X65M Grade, J. Fail. Anal. Prev. 13 (2013) 531–537.

[12] S. Mukhopadhyay, H.R. Jugade, G. Mukhopadhyay, S. Bhattacharyya. Failure Analysis of the Liner Plate of CDQ Chamber Made of AISI 310. Journal of Failure Analysis and Prevention. 15 (2015) 697-700.

[13] A. Abdollah-zadeh, M. Belbasy. Effects of Mn and Cu on the mechanical properties of a high strength low alloy NiCrMoV steel. Journal of Materials Science & Technology. 21 (2005) 470-474.

[14] C. Blais, G. LEsperance, H. Lehuy, C. Forget. Development of an integrated method for fully characterizing multiphase inclusions and its application to calcium-treated steels. Materials Characterization. 38 (1997) 25-37.

[15] F. Chen, Z. Cui, S. Chen, Recrystallization of 30Cr2Ni4MoV ultra-super-critical rotor steel during hot deformation. Part I: Dynamic recrystallization, Mat. Sci. Eng. A 528 (2011) 5073–5080.

[16] F. Chen, Z.S. Cui, D.S. Sui, B. Fu. Recrystallization of 30Cr2Ni4MoV ultra-super-critical rotor steel during hot deformation. Part III: Metadynamic recrystallization. Mat Sci Eng a-Struct. 540 (2012) 46-54.

[17] M. Mirzaee, H. Keshmiri, G.R. Ebrahimi, A. Momeni. Dynamic recrystallization and precipitation in low carbon low alloy steel 26NiCrMoV 14-5. Mat Sci Eng a-Struct. 551 (2012) 25-31.

[18] J.M. Barsom. A Study of Micro-cracks in Overheated Forgings of Ultra-Low Sulfur Steels for Aircraft Engine Crankshafts. (2009).

[19] J.L. He, Z.S. Cui, F. Chen, Y.H. Xiao, L.Q. Ruan. The new ductile fracture criterion for 30Cr2Ni4MoV ultra-super-critical rotor steel at elevated temperatures. Materials & Design. 52 (2013) 547-555.

[20] E.-J. Song. High Temperature Oxidation of Si-Containing Steel: Pohang University of Science and Technology; 2011.

[21] B.L. Bramfitt, A.O. Benscoter, Appendix: Tables Helpful to the Metallographer, Metallographer's guide: practice and procedures for irons and steels, ASM International, 2002, pp. 302-306.

[22] G.F. Vander Voort, Appendix I: Etchants for Revealing Microstructure (Pages 610-660), Metallography - Principles and Practice, ASM International, 1999, pp. 601-660.

[23] M. Opiela, A.Grajcar, Elaboration of forging conditions on the basis of the precipitation analysis of MX-type phases in microalloyed steels, Arch. Civ. Mech. Eng. 12 (2013) 427–435.

[24] R.W. Cahn, P. Haasen, Recovery and Recrystallization, Physical Metallurgy, North-Holland, 1996, pp. 2399-2482.

[25] D. Raabe, Recovery and Recrystallization: Phenomena, Physics, Models, Simulation, in: K.H. David E. Laughlin (Ed.), Physical Metallurgy, Elsevier, Oxford, 2014, pp. 2291-397.

[26] D.A. Porter, K.E. Easterling, Diffusionless Transformations, Phase Transformations in Metals and Alloys, T.J.Press, Great Britain, 1981, I992, pp. 422-5.

[27] Z. Yongtao, M. Lede, W. Xiaojun, Z. Hanqian, L. Jinfu. Evolution behavior of carbides in 2.25 Cr-1Mo-0.25 V steel. Materials transactions. 50 (2009) 2507-2511.

[28] M. Sohaciu, C. Predescu, E. Vasile, E. Matei, D. Savastru, A. Berbecaru. Influence of MnS inclusions in steel parts on fatigue resistence. Dig J Nanomater Bios. 8 (2013) 367-76.

[29] W.F. Gale, T.C. Totemeier, Diffusion in Metals, Smithells Metals Reference Book, Elsevier, 2004, pp. 920-1038.

[30] J. Robertson. The Mechanism of High-Temperature Aqueous Corrosion of Stainless-Steels. Corrosion Science. 32 (1991) 443-465.

[31] H.M. Tawancy, A. Ul-Hamid, N.M. Abbas, Corrosion, Practical Engineering Failure Analysis, CRC Press, 2004, pp. 379-385.

[32] S.E. Ziemniak, L.M. Anovitz, R.A. Castelli, W.D. Porter. Thermodynamics of Cr2O3, FeCr2 4, ZnCr2O4, and CoCr2O4. The Journal of Chemical Thermodynamics. 39 (2007) 1474-1492.

[33] R.W. Cahn, P. Haasen, Metallurgical Thermodynamics, Physical Metallurgy, North-Holland, 1996, pp. 429-434.

[34] S. Das, M. Mukherjee, T.K. Pal. Effect of grain boundary precipitation and delta-ferrite formation on surface defect of low nickel austenitic stainless steels. Engineering Failure Analysis. 54 (2015) 90-102.

[35] Z.H. Wang, S.H. Sun, B. Wang, Z.P. Shi, W.T. Fu. Importance and role of grain size in free surface cracking prediction of heavy forgings. Mat Sci Eng a-Struct. 625 (2015) 321-330.

[36] W.F. Hosford, Special Steels, Physical Metallurgy, CRC Press, 2010, pp. 319-327.

[37] T. Reza, N. Abbas, S. Reza. Drawing of CCCT diagrams by static deformation and consideration deformation effect on martensite and bainite transformation in NiCrMoV steel. Journal of Materials Processing Technology. 196 (2008) 321-331.

Table captions

C	Ni	Cr	Mn	Mo	Si	V	Cu	Al	S	N	AlxN
0,30	2,66	1,44	0,36	0,35	0,22	0,095	0,13	0,014	0,005	0,0037	$5{,}2.10^{-3}$

Table 1 : The chemical compositions of the studied steels (wt.%)

Zones	Depth from surface (mm)	ASTM grain size	Average diameter of grains (µm)
S1	0	1	250
S2	85	6,5	35
S3	0	-1	550
S4	0	-0,5	425

Table 2 : grains size reported on different zones of samples

Figure captions

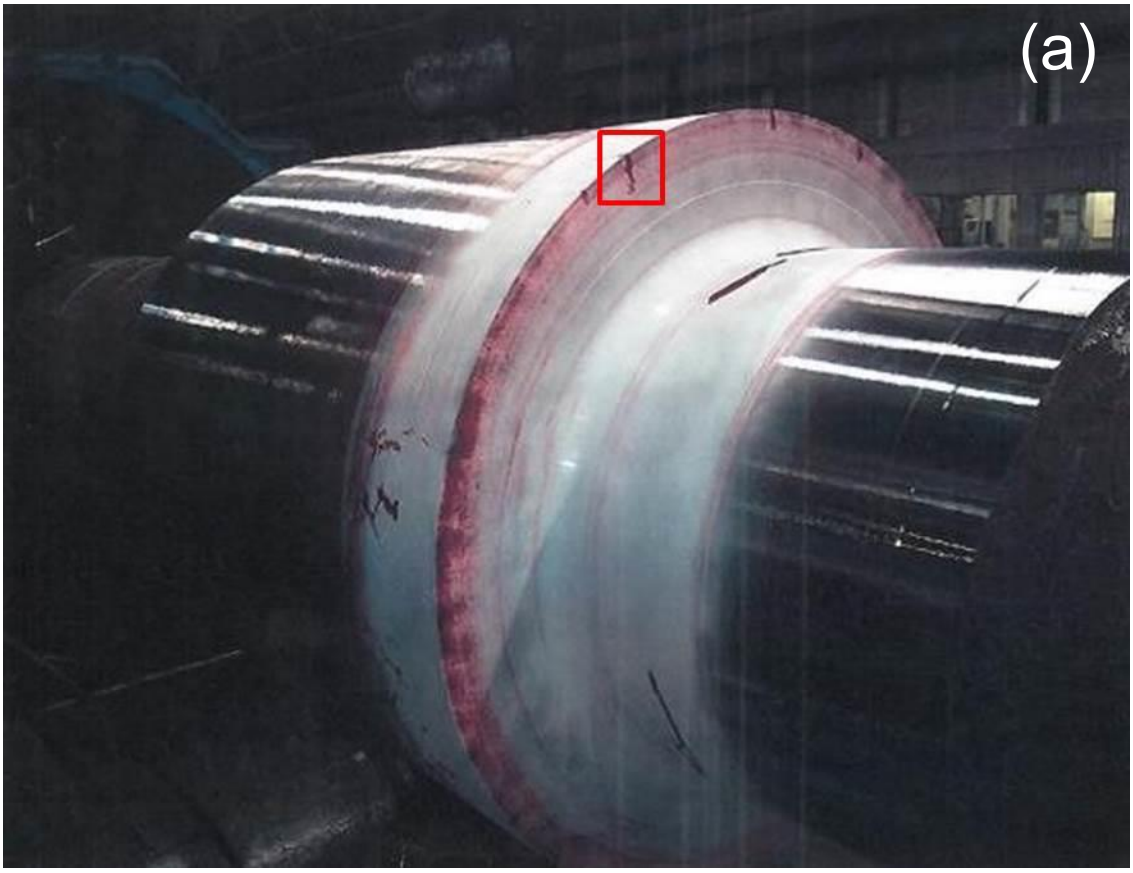

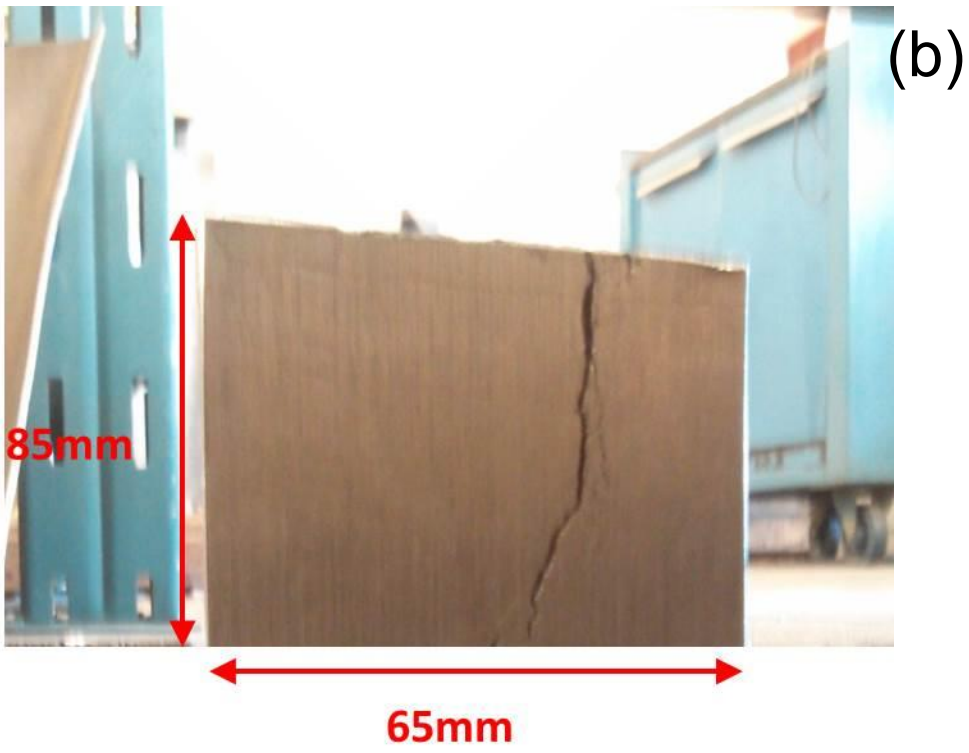

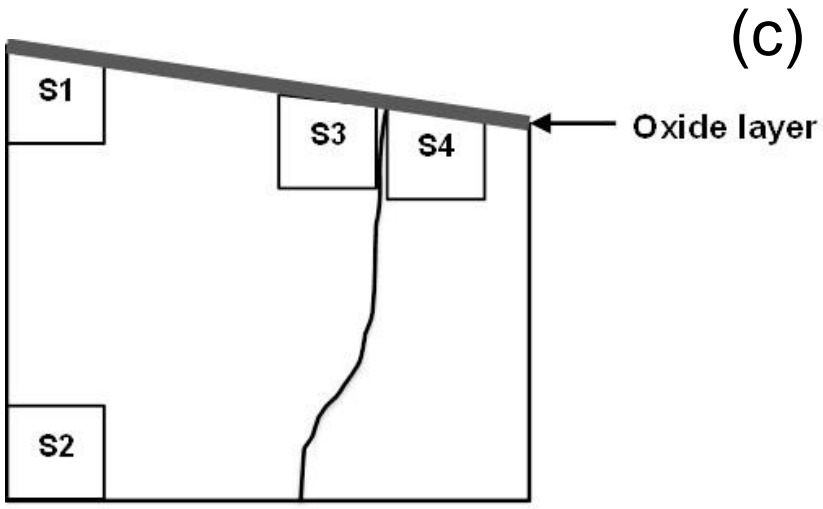

Fig. 1 : (a) Penetrant testing on the forged ingot showing cracks, and surface sample taken for the study, (b) Dimensions and apparition of a main crack on the sample, (c) Specimens cut from the sample for grain size and metallographic analyses

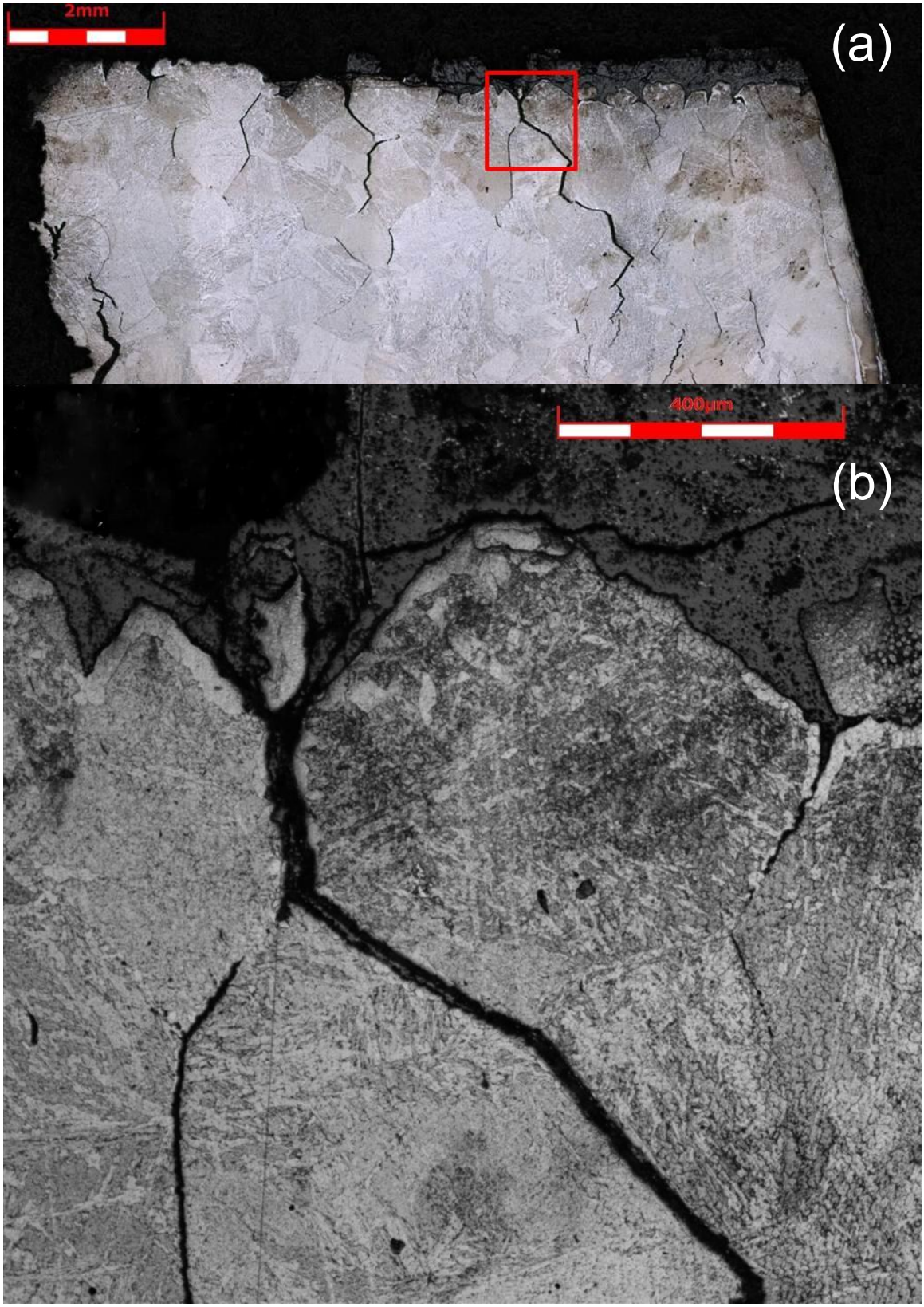

Fig. 2 : (a) S4 sample surface micrograph, (b) oxide following grain boundaries

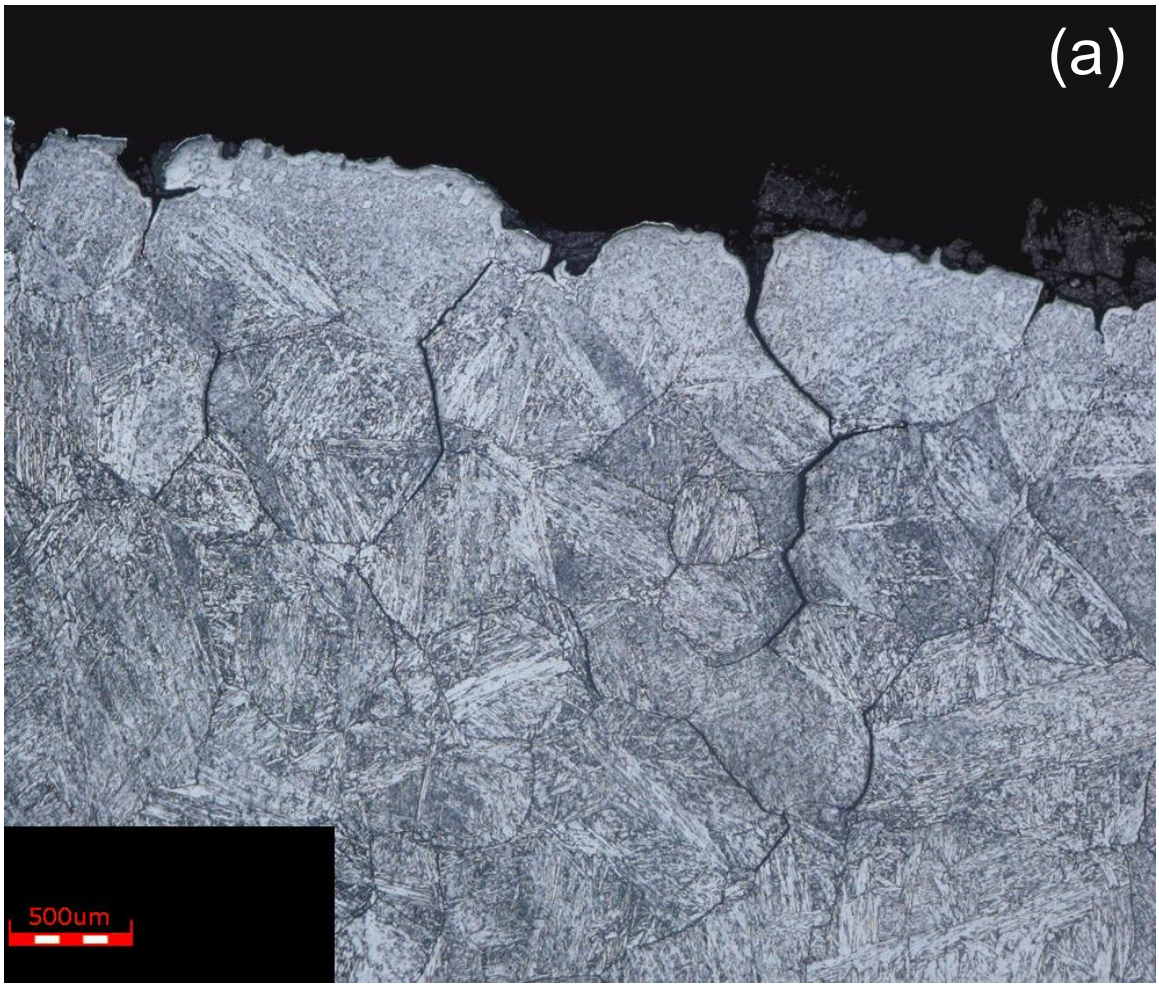
(a)
500um

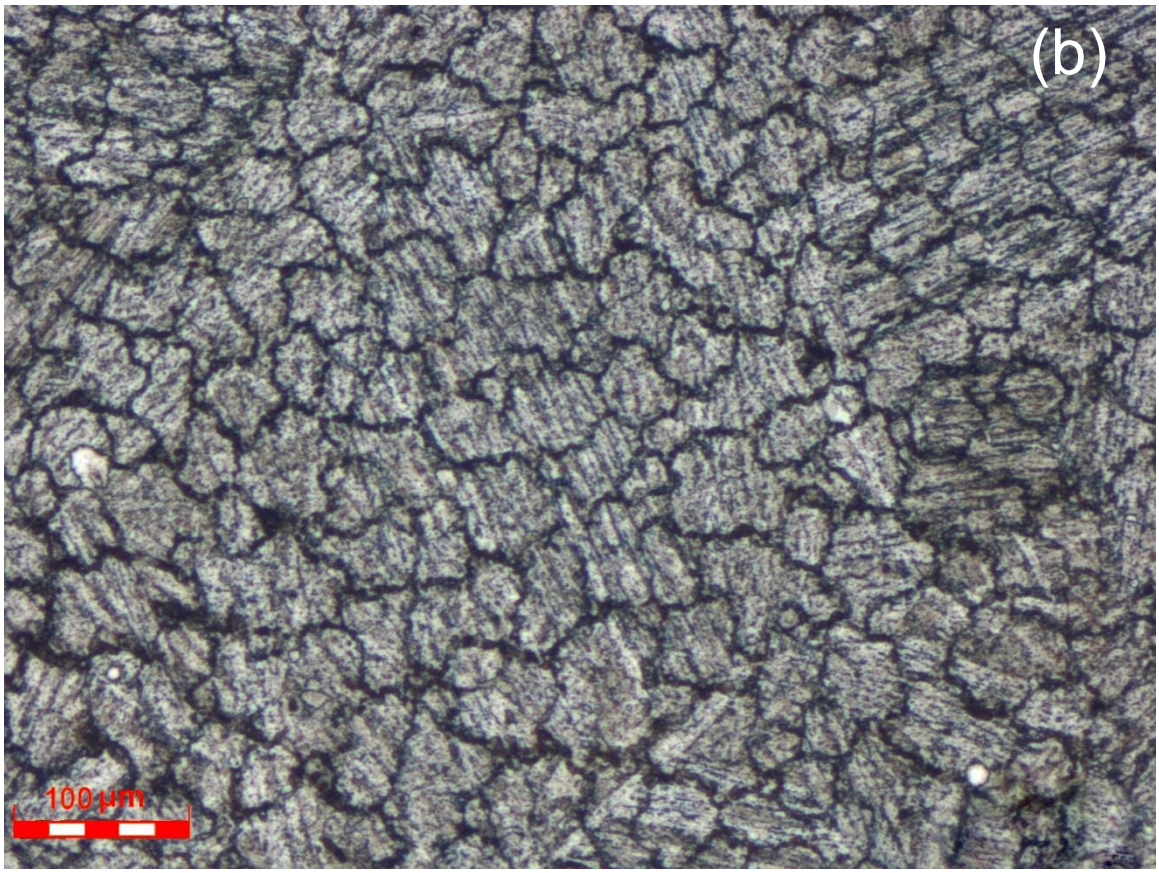

Fig. 3 : (a) Microstructures and cracks observed on the surface of the S4 specimen, (b) grain size in S2 specimen

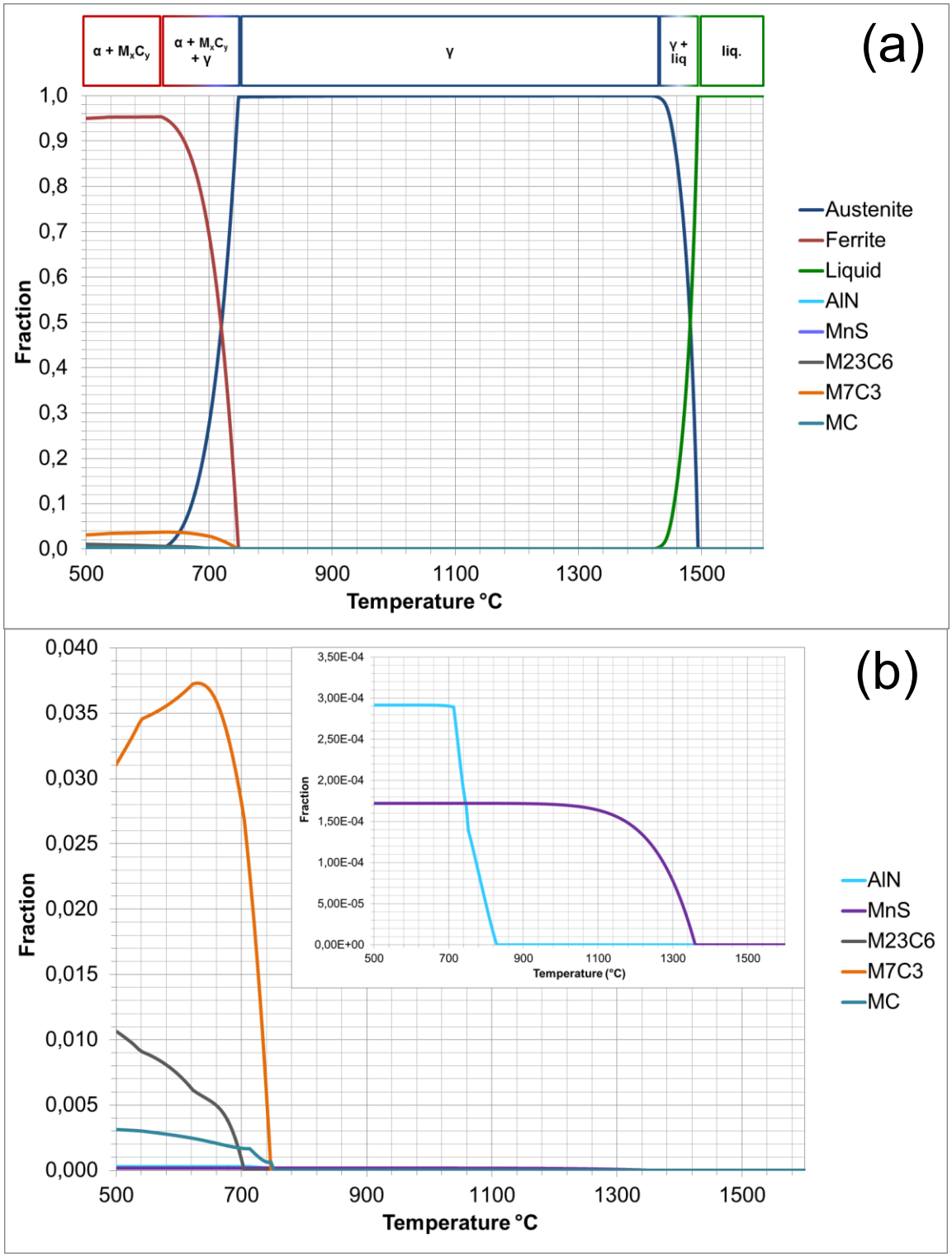

Fig. 4 : Thermo-Calc simulation between 500 and 1600°C using composition of Table 1, (a) whole simulation, (b) Close-up on precipitates proportions

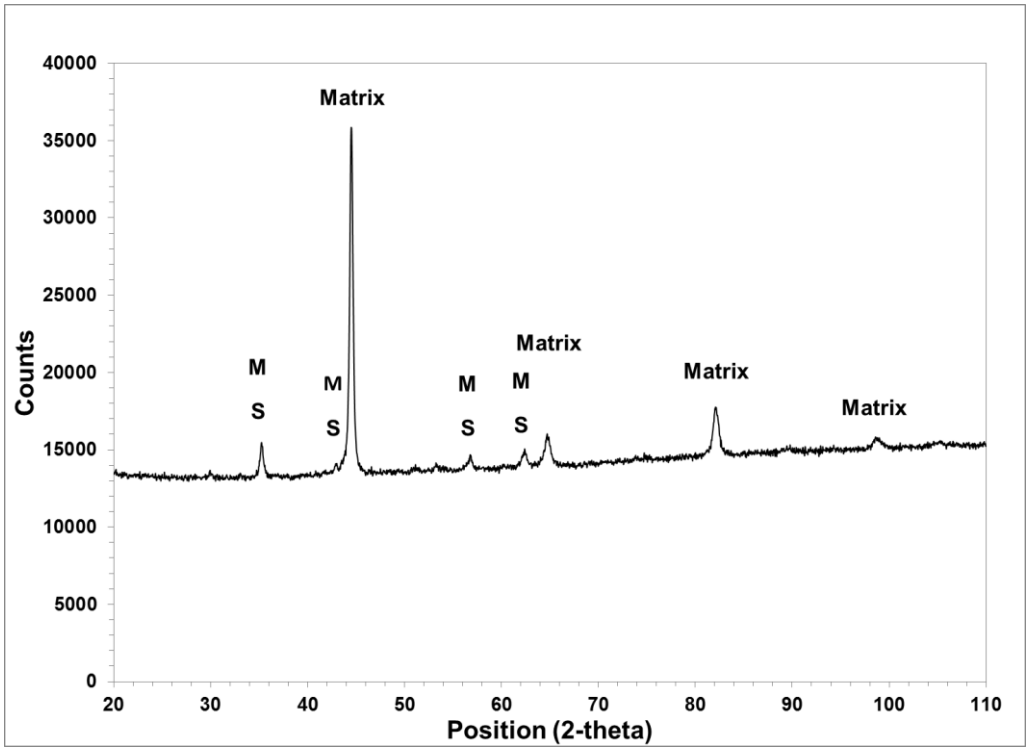

Fig. 5 : X-ray diffraction of the interface of the oxide layer and steel; M and S stand for Magnetite (Fe_3O_4) and Spinel ($NiFe_2O_4$) respectively.

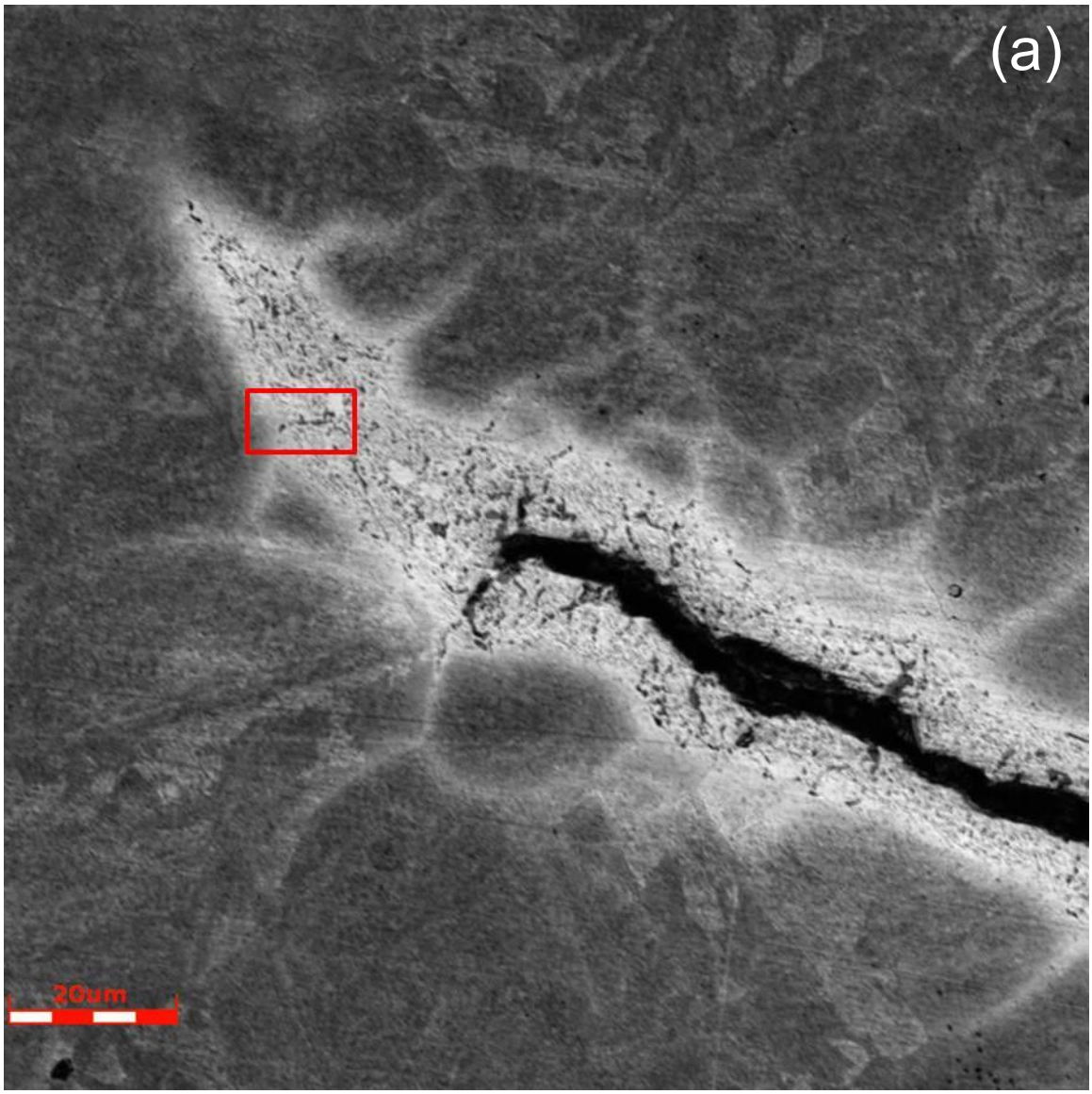
(a)
20um

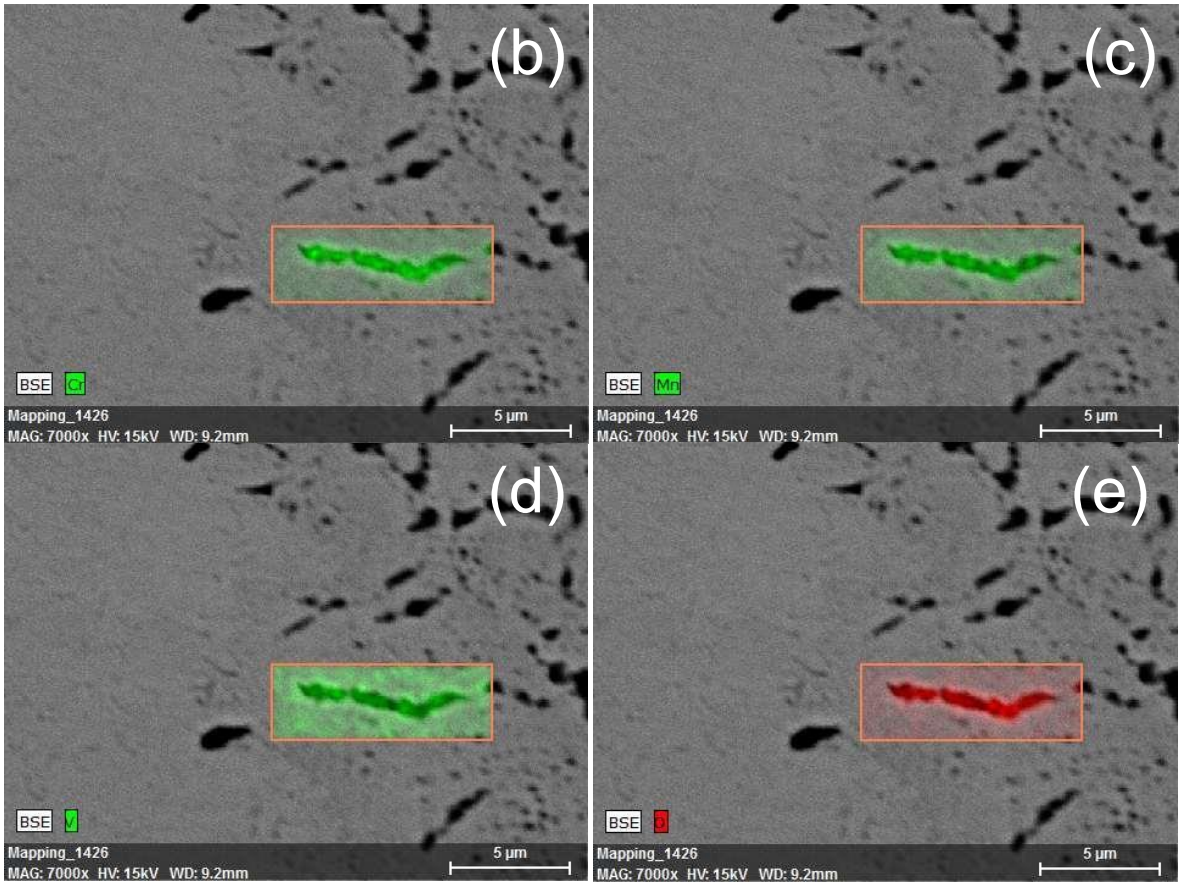

Fig. 6 : EDS analysis of an inclusion at the base of a crack. Microstructure was revealed with Beaujard reagent. (a) Base crack, (b)(c)(d)(e) Cr, Mn, V and O presence on precipitate close to the crack surface.

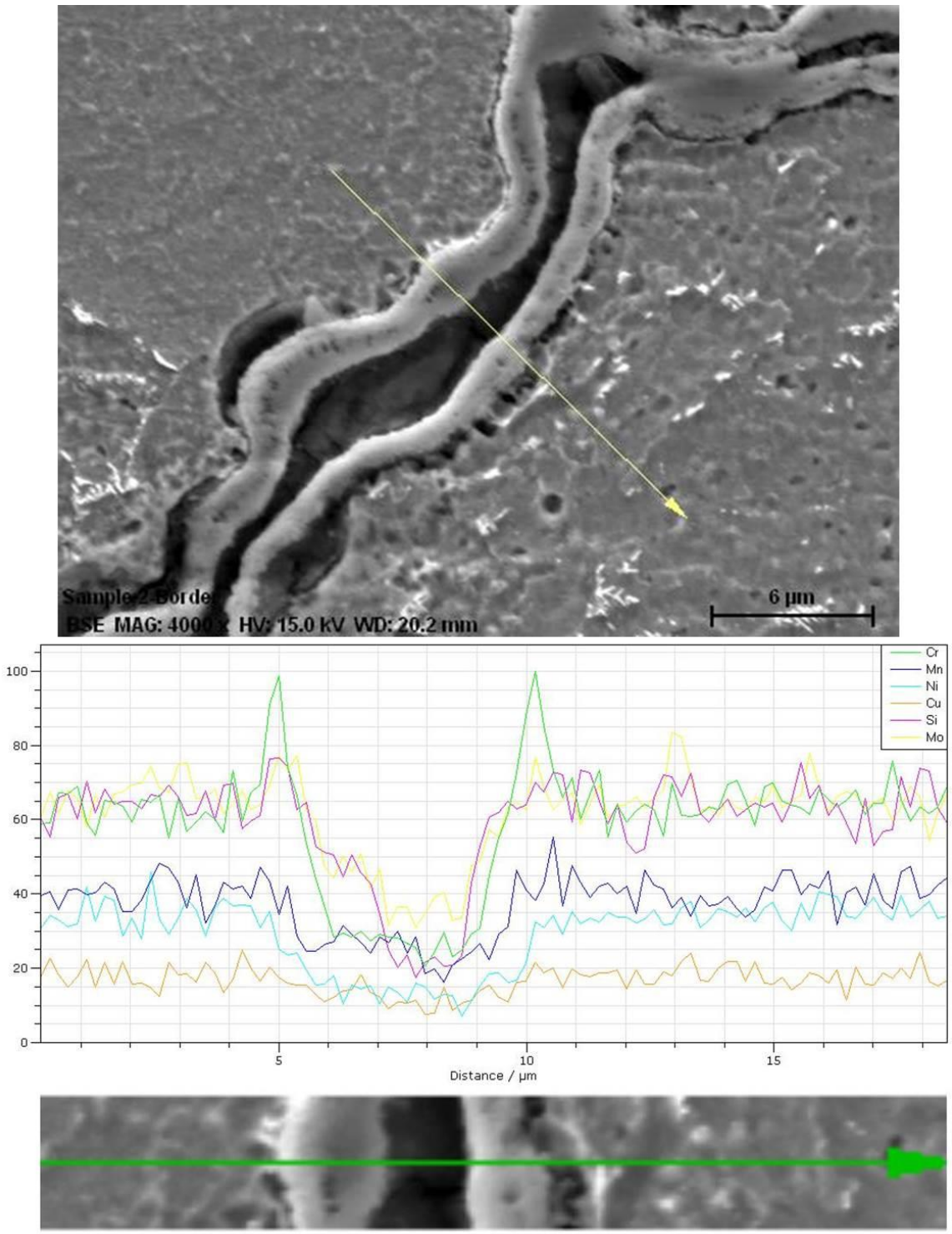

Fig. 7 : Cross-section EDS analysis of a crack, showing the unique presence of chromium in oxide layer